

An approach for radiation dose reduction in computerized tomography

Shama Bekal Narayan, Savitha Halkare Mahabaleshwara

Department of Electronics and Communication Engineering, Faculty of Engineering, St Joseph Engineering College, Mangalore, India

Article Info

Article history:

Received Feb 2, 2022

Revised Sep 23, 2022

Accepted Oct 8, 2022

Keywords:

Hardware

Image

Radiation

Software

X-ray

ABSTRACT

Minimization of radiation dose plays an important role in human wellbeing. Excess of radiation dose leads to cancer. Radiation greatly affects young children less than 10 years of age as their life span is longer. Radiation can be reduced by hardware and/or by software techniques. Hardware methods deal with variation of parameters such as tube voltage, tube current, exposure time, focal distance and filter type. Software techniques include image processing methods. The originally acquired X-ray images may be contaminated with noise due to the fact of instability in the case of sensors, electrical power or X-ray source, that is responsible for the degradation of the image attributes. An enhanced image denoising algorithm has been proposed which decreases Gaussian noise combined with salt and pepper noise that retains most information particulars.

This is an open access article under the [CC BY-SA](https://creativecommons.org/licenses/by-sa/4.0/) license.



Corresponding Author:

Shama Bekal Narayan

Department of Electronics and Communication Engineering, Faculty of Engineering, St Joseph Engineering College, Affiliated to Visveshwaraya Technological University

Vamanjoor, Mangalore, Karnataka 575028

Email: shamabn@sjec.ac.in

1. INTRODUCTION

Diagnostic examination is a medical specialty procedure which involves medical procedures to identify and treat diseases. Non-invasive methods like X-ray radiography and computed tomography (CT) are used to diagnose or treat diseases. The X-rays pass across the human body, creating a computer display. Direct digital radiography produces an image instantly on a computer screen. Radiologists can access the image quickly. CT uses X-rays to recognize and note the radiation absorbed by different organs. Radiology technicians/doctors use these images to analyze bone fractures and other illnesses in the human body [1].

These medical examinations present both benefits and threats. The benefits of these examinations far exceed the risks. They are fast, painless and non-invasive. Examinations provide detailed information to identify the issue, treatment plan, and assess many complications in adults and children. In addition, the accurate images provided by CT scans may waive off the surgery [2]. Dental radiology plays a vital role in pediatric patients. Recognizing the variety of retraction of chin is critical for distinct investigation in research. Dentofacial skeletal features differ based on the type of malocclusion [3]. The investigation done on the juvenile idiopathic arthritis (JIA) recommends children and youngsters are influenced with unilateral or bilateral balanced to serious temporomandibular joint (TMJ) issues [4]. The cephalometric X-ray supports the dentist to acquire an entire radiographed picture of the side of the face. Cephalometric regularizing quantum values for the 8-to-12-year-old South Italian children population was referred to in study. Important characteristic features among boys and girls in the range of the anterior cranial base and ratio obtained are recorded [5].

Reducing the radiation helps in reducing the risk of cancer. Radiation can be reduced by using hardware and software techniques. Hardware approaches include the analysis of five exposure parameters and software approaches involve implementation of distinct algorithms. The exposure to ionizing radiation may lead to a slight raise in an individual's lifetime risk of originating malignancy or cancer [6]. As a person is exposed to radiation, risk of developing cancer also increases. Risk is greater in children's as they have longer life spans. Possibility of raising cancer boosts with periodic subjection to diagnostics imaging methodologies. Probability is twofold in case of expecting mothers and in offspring. A baby in the womb may also be more sensitive to radiation than an adult. Scientific research facilitates better evaluation of the risks. It is observed that as years pass on radiation dose is reduced. Dose can be reduced by both hardware and software techniques. Hardware techniques include five important exposure confines namely tube voltage (kV), tube current (mA), exposure time (ms), focus to detector distance (cm) and filter type. Software approach involves distinct algorithms. Aim is to minimize noise and import clarity to the image by applying rebuilding techniques and required filters. If the clarity in image is good, doctors can diagnose the issue of patients. If the image is clear then radiation dose can be reduced. Objective is: i) To reduce radiation dosage in X-ray, especially for pediatric use and reduce the risk of cancer; ii) To develop an improved image filtering algorithm to support the reduction of radiation dose; iii) To identify and filter the various noises present in images; and iv) To enhance the images for scene visibility, enhance the contrast and edges in the X-ray images. Scope includes long term health benefits to individuals, health benefits to Oncology patients who are exposed to radiation therapy, in future, state of art algorithms can be implemented by X-ray manufactures such as Siemens, Philips and General Electric (GE) for health care application.

2. METHOD

Radiation dose reduction [7] follows two major approaches. Hardware and software methods [8]. Figure 1 illustrates different approaches to radiation reduction. Hardware technique includes modification in the geometry of X-ray machines. As per data sheets of top medical device manufacturing company, Radiation induced depends on tube voltage in Kilovolts, tube current in milliamperes, exposure time in milliseconds, prefilter, and focal spot.

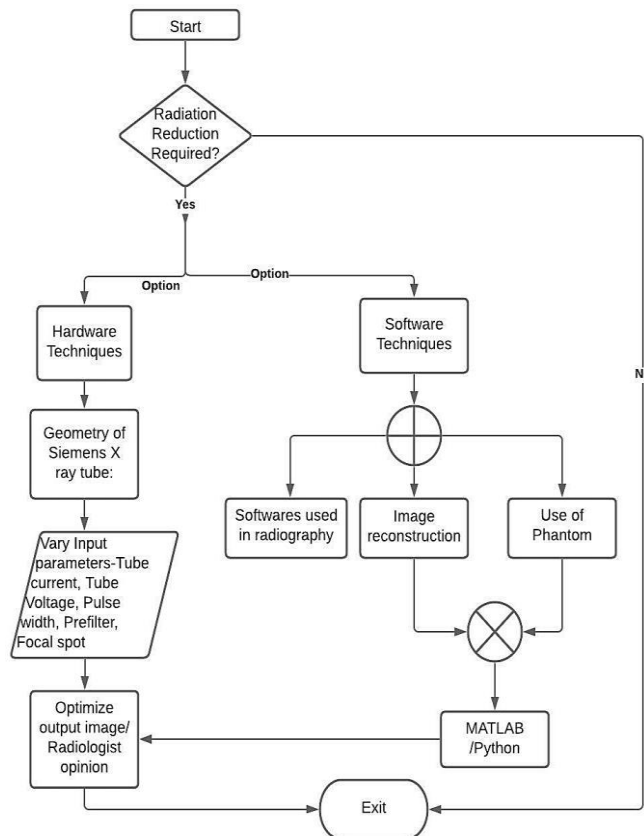


Figure 1. Flowchart - techniques of radiation dose reduction

Radiation builds on a patient body mass index. Radiograph energy is directly proportional to patient thickness. Reputed medical device manufacturing company has inbuilt automatic exposure control adjustments. To analyze these algorithms, one needs to have an X-ray machine with access to the gateway of network.

A graphical user interface (GUI) based LabVIEW approach is used to implement body mass index calculations. If the body mass index is greater than the threshold, radiation dose increases. Caldose software program is used to calculate radiation dose induced in different parts of the body for a specific X-ray profile. Chest X-ray profile is selected for study because chest x ray is most frequently performed examination, according to annual frequency of examination conducted during 2002 [8].

Different software's were tried to reduce radiation dose. Some of them are Imasim, Mevislab, Analyze 14.0, Code_Blocks, Git bash, medical image processing, analysis, and visualization (MIPAV), DOSCTP/DOSXYZnrc. Many radiology-based apps were studied for the purpose of radiation dose reduction. Software Techniques include removing noise in image by the use of various filters. As radiation is reduced image becomes blurry. Hence it is ideal to minimize the noise in the X-ray image.

Data for analysis was collected from a private hospital. Two technicians were involved from renowned healthcare technology management services. Inclusion criteria comprise general patients requiring X-ray diagnosis. Oncology patients were excluded from the study. Statistical methods for noise analysis include different types of filtering along with advanced image denoising algorithms.

3. TECHNIQUES IMPLEMENTED

3.1. Hardware techniques

Radiation exposure can be controlled by using hardware techniques. External parameters can be varied for different setups for analysis purposes. LabVIEW and Caldose software were used for implementation. Different methods of hardware techniques tried is as follows:

3.1.1. White paper of top medical device manufacturing company

According to medical device manufacturing company's white paper [9], Radiation dose is calculated based on patient size, density of anatomical area irradiated and C-arm regulation of x ray tube. Radiation dose also depends on Tube voltage (kV), Tube current (mA), Exposure time (mS), Focal spot and pre-filter (CARE filter).

As per the analysis, radiation dose cannot be reduced in already deployed machines. Image processing was done using C++. Objective of research mainly deals with hardware [10] control. Radiation builds on a patient body mass index. Radiograph energy is directly proportional to patient thickness. Reputed medical device manufacturing company has inbuilt automatic exposure control adjustments. To analyze these algorithms, one needs to have an X-ray machine with access to the gateway of network.

3.1.2. LabVIEW

Implementation of body mass index (BMI): Radiation dose depends on patient thickness. Calculation of BMI for pediatric patients is implemented using LabVIEW as per Figure 2. Radiation dose increases with BMI. Radiation dose needs to be adjusted with BMI. Implementation of radiation reduction was tried in LabVIEW. Three hardware parameters were considered namely tube voltage, tube current and exposure time. Hounsfield units using the (1).

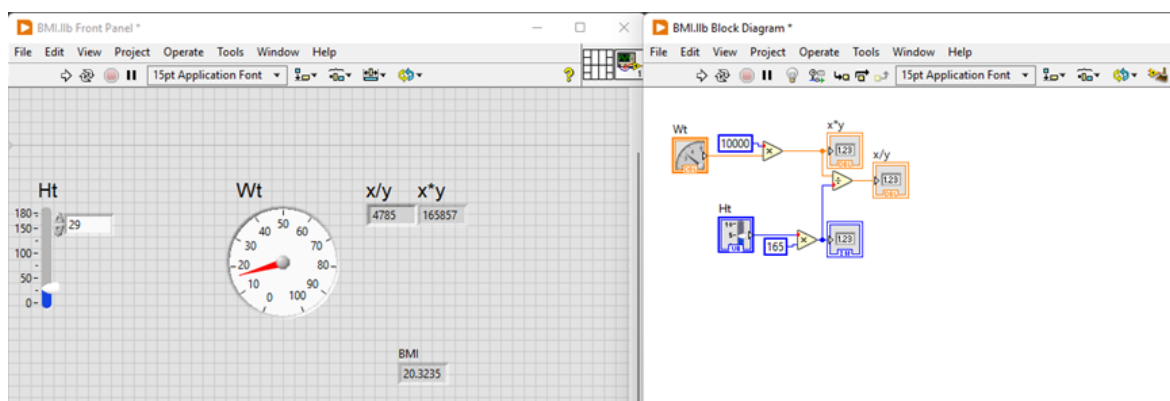


Figure 2. Implementation of BMI using LabVIEW

$$HU = \frac{(\mu_{material} - \mu_{water})}{(\mu_{water})} \times 100 \quad (1)$$

Different substances like air, fat, soft tissue and bone were implemented using case structures. Figure 3 shows an approach for radiation reduction-Hounsfield scale, using LabVIEW. But implementation was misfired.

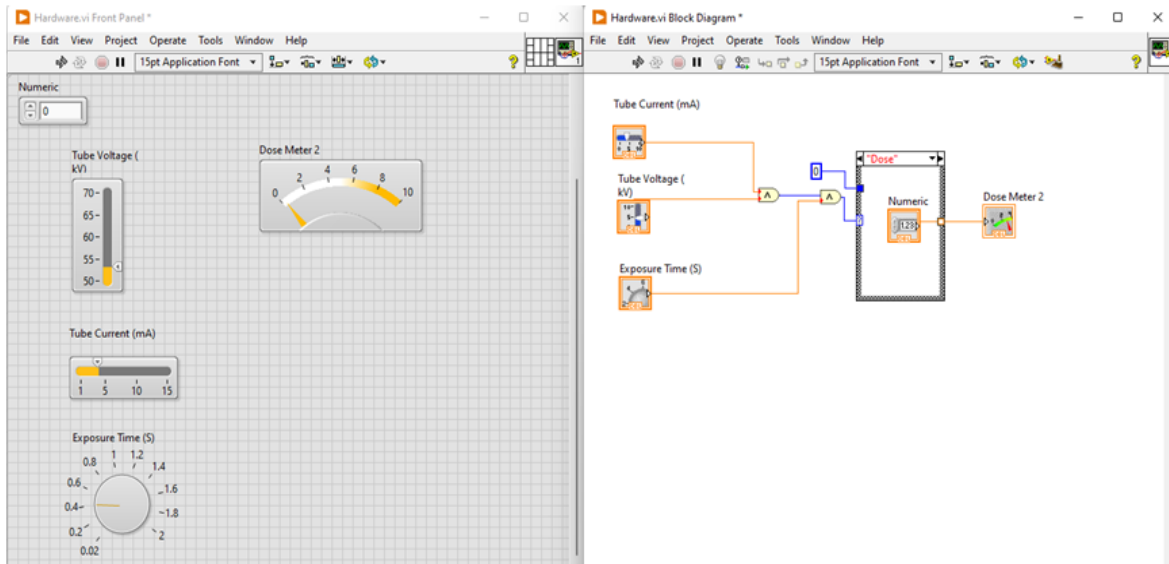


Figure 3. Radiation reduction using in LabVIEW using Hounsfield scale: declined

3.1.3. CalDose

CALDose_X 5.0 is the current version of a software program for X-ray diagnosis. It is used for calculating organ absorbed doses and radiological risks. Figure 4 shows two human adult phantoms male adult mesh (MASH) and female adult mesh (FASH). Clean and clear concept of radiation dose reduction is implemented using Caldose. Figure 5 implies X-ray examination with different values of film-focus distance (FFD), kv and mAs.

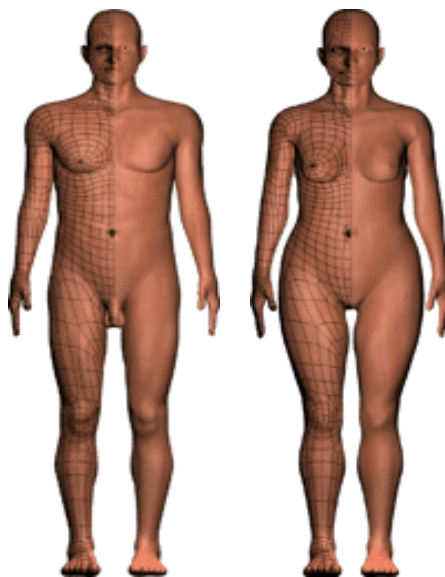


Figure 4. Two human adult phantoms

Definition of the X-Ray Examination

INSTITUTION:

ROOM:

ADULT PATIENT

Name:

ID: Age (years):

Female Standing

Female Supine

Male Standing

Male Supine

EXAMINATIONS

PROJECTIONS

Anterior-Posterior (AP)

Posterior-Anterior (PA)

Right Lateral (RLAT)

Left Lateral (LLAT)

Right Posterior Oblique (RPO)

Left Posterior Oblique (LPO)

Right Anterior Oblique (RAO)

Left Anterior Oblique (LAO)

X-RAY TUBE (Filter: 2.5 mm Al)

120 ≤ FDD ≤ 220 (cm) Charge (mAs) 60 ≤ Voltage ≤ 150 (kV)

FIELD POSITIONS

Standard field position

Standard field + 2 cm up

Standard field + 2 cm down

Calculate INAK?

Yes

No

X-RAY TUBE OUTPUT (Filter: 2.5 mm Al)

Number of Points

X-Ray Tube Identification

Air KERMA x Potential	
Potential (kV)	K (μGy/mAs at 1 m)
50	41.29
60	60.93
70	80.98
80	102.42
90	125.16
100	148.85
110	173.32

Figure 5. X ray examination with FFD, mAs and kV

3.2. Software techniques

As radiation is reduced the image becomes blurry [11]. Radiologists find it difficult to diagnose the complications in the patient’s X-ray. Because of hardware restrictions and practical issues, it is impossible to reduce dose. Low dose CT [12] with image clarity is a challenge. Aim is to identify different noise in X-ray image, reduce noise in image and enhance image characteristics using different image processing techniques [13].

Model based Iterative reconstruction techniques [14] with high performance [15] and graphics processing unit [16] are some of the reconstruction [17] techniques recently used for chest X-ray used in medical imaging [18]. Filtered back projection [19] technique solves the issues of blurring. Deep learning methods [20] can be used for image reconstruction. Convolutional neural networks play an important role in radiation reduction [21].

The design is based profoundly on the seed particle. By dividing the image in various fragments, each and every single pixel value of the image is contrasted with respect to a particular threshold value determined in consideration to the gray value of the seed point [22].

- a. Take a pixel in the initial input image and specify it as a seed particle. Place the particular seed pixel value toward a blank progression.
- b. Since the beginning of the progression, find consequent 8- associated neighbors of every pixel which are not processed and for every neighbor point, see if the gray zone value of that neighbor particle is in the range of the stated discrepancy from the seed particle’s gray zone value. This discrepancy is illustrated by (2).

$$\frac{(f(x,y)-seed)}{seed} \leq \epsilon \tag{2}$$

Here, $f(x, y)$ is the gray zonal value of the current particle and ϵ is the origin value equal to 0.5.

- c. Thirdly, the foreground section is further improved by adjusting the histogram accordingly and is summed up to the background section.
- d. Lastly, an improved image is produced by combining the grade of the initial image to the image obtained in the C step.
- e. On the basis of the seed point which is taken, the entire image is divided into foreground and background sections.

4. RESULTS AND DISCUSSION

4.1. Results of hardware approach

Figure 6 gives a plot of potential versus air kerma. Figure 7 shows the beam position of chest X-ray. Air kerma also increases with Potential. X-ray source reaches the detector through the sample.

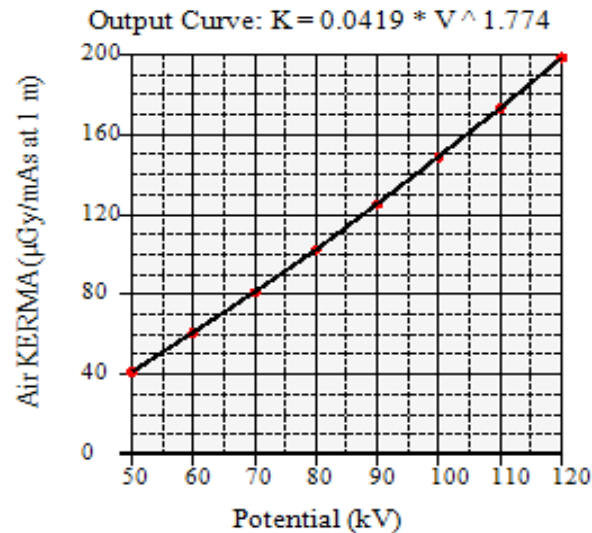


Figure 6. Plot of potential versus air kerma

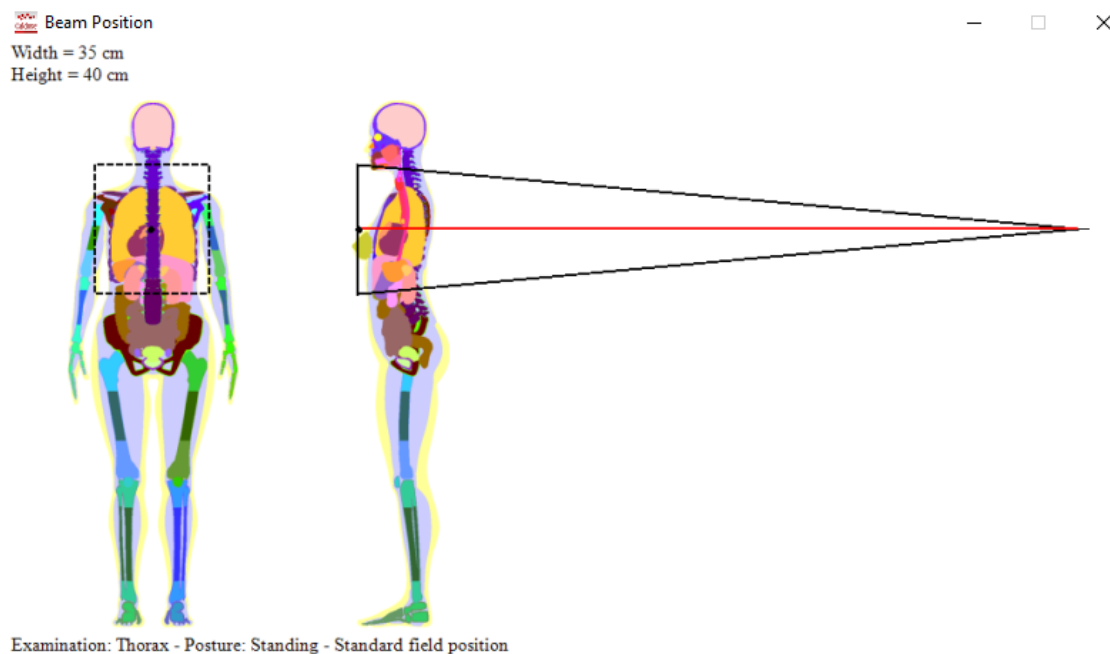


Figure 7. Beam position of chest X-ray

Figure 8 shows the dose analysis chart for FFD=220 cm, tube voltage = 150 kV and tube current and exposure time product value 24 mAs. Figure 9 demonstrates dose analysis chart for variations in FFD. Absorbed dose is calculated for different organs. X-ray parameters are varied for analysis purpose.

Figure 10 shows dose comparison chart with min and max FFD, constant mAs and kV. Figure 11 implies a dose comparison chart for min and max values of FFD, mAs and kV. Figure 12 dose comparison with the variation of FFD, mAs and kV. Absorbed dose is calculated for different organs. X-ray parameters are varied for analysis purpose.

Dose Analysis for FDD=220cm, Tube current exposure time product value = 24mAs and Tube Voltage = 150kV

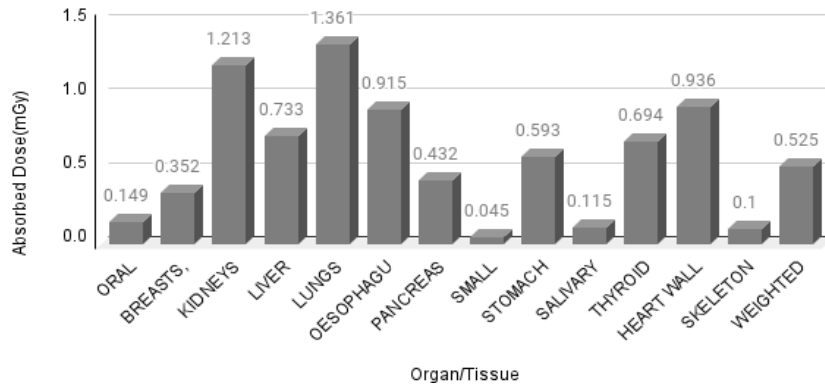


Figure 8. Dose analysis chart for FFD=220 cm, tube voltage = 150 kV and tube current and exposure time product value 24 mAs

Dose Analysis chart for variations in FDD

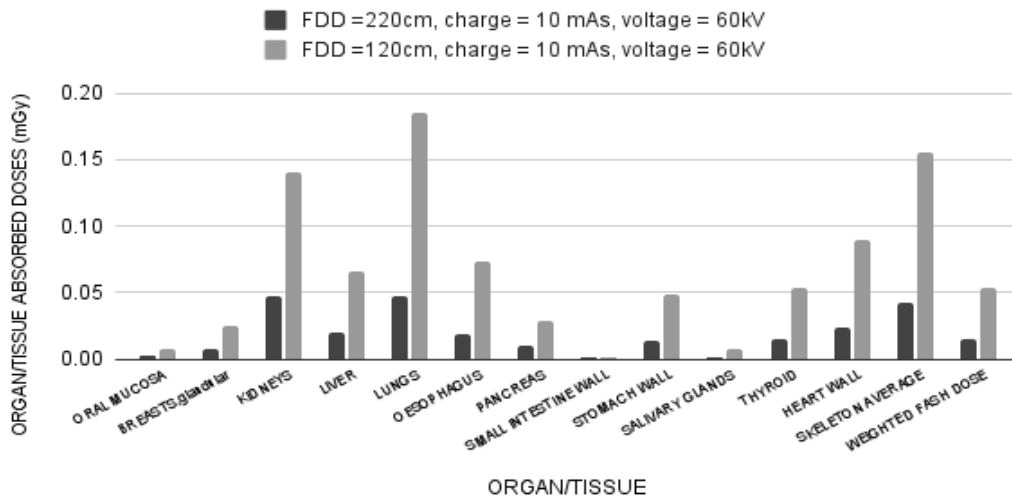


Figure 9. Dose analysis chart for variations in FFD

Dose comparison at Min and max FFD, with constant mAs and kV

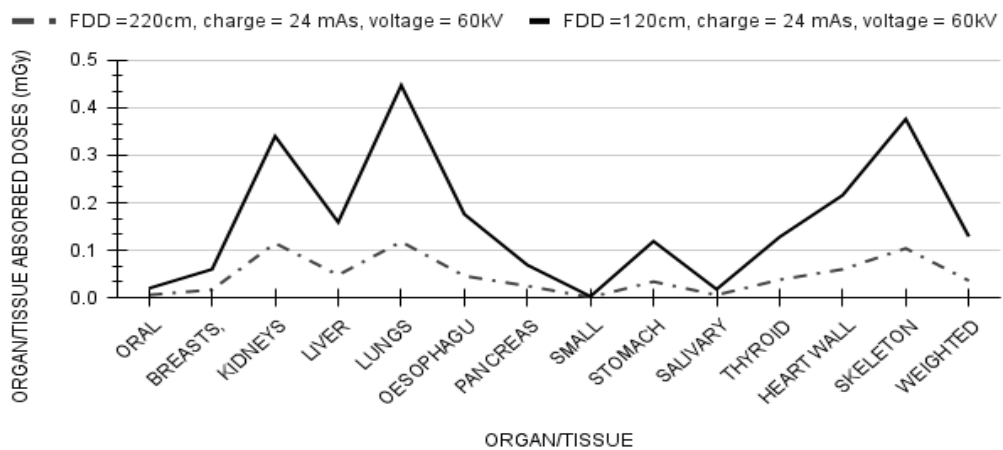


Figure 10. Dose comparison chart with min and max FFD, constant mAs and kV

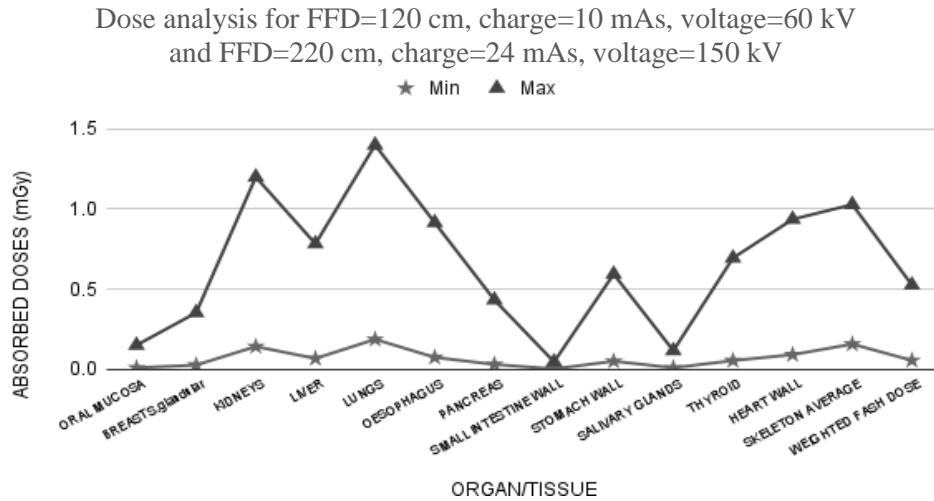


Figure 11. Dose comparison chart for min and max values of FFD, mAs and kV

Dose comparisons with the variation of FDD, mAs and kV

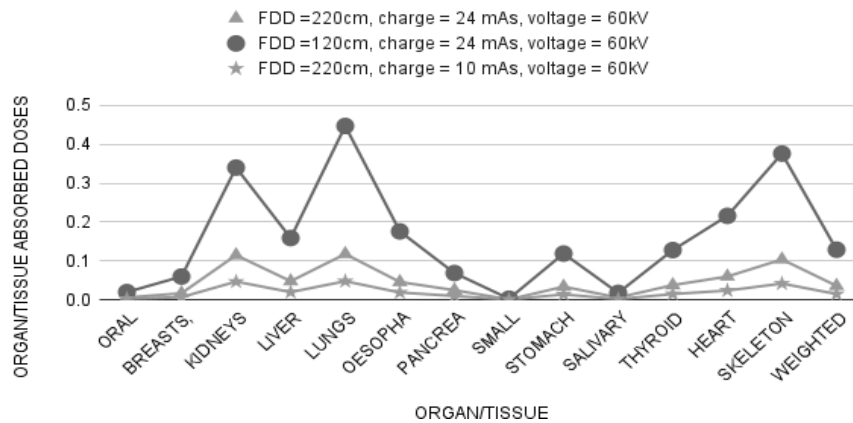


Figure 12 Dose Comparison with the variation of FFD, mAs and kV

4.2. Results of software approach

Software approaches were divided into 3 cases. Case 1 was analyzed when X-ray is contaminated with Gaussian noise. Figure 13 shows the input X-ray image contaminated with Gaussian noise. Figure 14 shows the output of the filter. Figure 15 shows an enhanced output image. Case 2 was analyzed when X-ray is contaminated with salt and pepper noise. Figure 16 shows the input X-ray image contaminated with salt and pepper noise. Figure 17 shows the output of the filter. Figure 18 shows an enhanced output image. Case 3 was analyzed when X-ray is contaminated with both Gaussian and salt and pepper interference. Figure 19 shows the input X-ray image contaminated with both Gaussian and salt and pepper interference. Figure 20 shows the output of the filter. Figure 21 shows an enhanced output image.

The innovative noise reduction technique which involves median filtering along with threshold filtering obtained greater signal-to-noise ratio (SNR) and peak signal-to-noise ratio (PSNR) values but, however lower mean squared error (MSE) value [23]. This indicates that the novel interference reducing algorithm which diminishes the interference than traditional procedures still maintain better visual details. The human conception is no longer treated as a standard for the image quality, and therefore to estimate the conduct of the proposed design, quality parameters were measured such as contrast to noise ratio (CNR), SNR, PSNR, and MSE.

In hardware techniques, as focus to detector distance is increased dosage is reduced. Tube voltage, tube current and exposure time [24] product value has to be minimum. Different algorithms can be used for fast image processing, [25] which can be used for fluoroscopic applications [26]. Various CT reconstruction [27] techniques may contribute to future work.

CASE 1: when the X-ray is contaminated with Gaussian noise

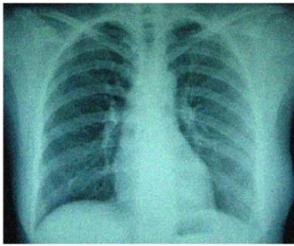


Figure 13. Input X-ray image contaminated with Gaussian noise

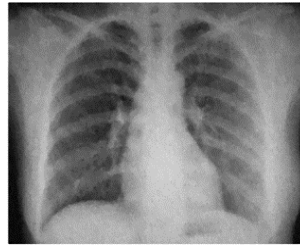


Figure 14. Filtered radiograph image

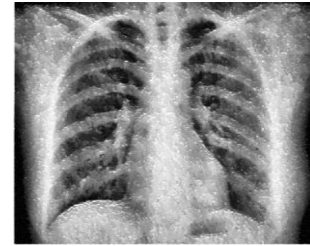


Figure 15. Filtered and enhanced output radiograph image

CASE 2: when the X-ray is corrupted with salt and pepper noise

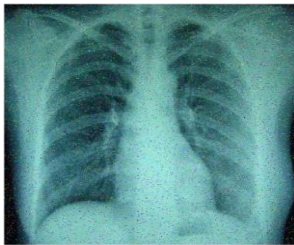


Figure 16. Input X-ray image corrupted with salt and pepper interference

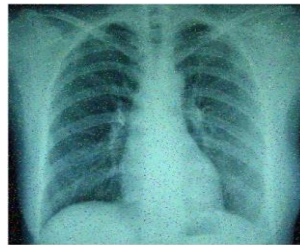


Figure 17. Filtered radiograph image



Figure 18. Filtered and enhanced output radiograph image

CASE 3: when the radiograph is contaminated with both Gaussian and salt and pepper interference

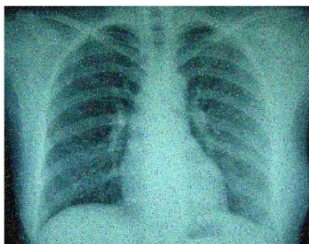


Figure 19. Input radiograph image corrupted with both Gaussian, and Salt and Pepper interference



Figure 20. Filtered radiograph image

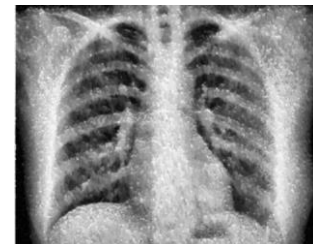


Figure 21. Filtered and enhanced output X-ray image

5. CONCLUSION

Hardware Techniques implies that radiation dose can be reduced by increasing focus to detector distance. Tube voltage, Tube current and exposure time product value has to be minimum and ensure quality image is retained. Future work deals with the study of copper filters. Aluminum filters are used in most of the X-ray machines. Copper filters reduce the radiation dose. In software techniques, the originally acquired X-ray images are contaminated with noise due to the fact of instability in the case of sensors, electrical power or X-ray source, that is responsible for the degradation of the image attributes such as submerging valuable information, and blurring edges. Here an enhanced image denoising algorithm has been proposed which decreases Gaussian noise combined with salt and pepper noise that retains most information particulars.

In comparison of this method with the currently prevalent methods of flexible improvement and fine stretching and other contrast enhancement techniques, it is summarized that this innovative technique is exhibiting much better and improved outcomes than the currently prevalent ones. Moreover, the method is seed-dependent and therefore the determination of seed particles is very much vital in this design. A seed selected in dark sections will yield improved outcomes compared to the seed selected in the bright sections, as it is expected that the enhancement of the darker regions of the image is required.

Also, the innovative enhancement technique can also be combined with adaptive enhancement Method to produce outputs with still better results and improved perception. Hard problems include radiation dose reduction by adjusting the X-ray machine settings. Adjusting the settings of an X-ray machine is a challenge. This has to be done by the X-ray machine manufacturers. Non obvious mistakes include collection of data from the hospital instead of contacting the technician of the X-ray machine.

ACKNOWLEDGEMENTS

Author thanks guide Dr. Dayakshini, Head of ECE Department, Dr. Rio D Souza, Principal, and St Joseph Engineering College for their guidance during my research work. Author would like to express sincere gratitude to the management of St Joseph Engineering College for constant support.





REFERENCES

- [1] ITN, "Radiology imaging, imaging technology news," *Imaging Technology News*, <https://www.itnonline.com/channel/radiology-imaging/Radiation> (accessed Dec. 12, 2020).
- [2] FDA, "Computed tomography, US food drug administration." *US Food and Drug Administration*. <https://www.fda.gov/radiation-emitting-products/medical-imaging/medical-x-ray-imaging> (accessed Aug. 08, 2020).
- [3] L. Perillo, G. Padricelli, G. Isola, F. Femiano, P. Chiodini, and G. Matarese, "Class II malocclusion division 1: a new classification method by cephalometric analysis," *European Journal of Paediatric Dentistry*, vol. 13, no. 3, pp. 192–196, 2012.
- [4] G. Isola, L. Ramaglia, G. Cordasco, A. Lucchese, L. Fiorillo, and G. Matarese, "The effect of a functional appliance in the management of temporomandibular joint disorders in patients with juvenile idiopathic arthritis," *Minerva Stomatologica*, vol. 66, no. 1, pp. 1–8, 2017, doi: 10.23736/S0926-4970.16.03995-3.
- [5] L. Perillo, G. Isola, D. Esercizio, M. Iovane, G. Triolo, and G. Matarese, "Differences in craniofacial characteristics in Southern Italian children from Naples: a retrospective study by cephalometric analysis," *European Journal of Paediatric Dentistry*, vol. 14, no. 3, pp. 195–198, 2013.
- [6] A. Berrington de González, "Projected cancer risks from computed tomographic scans performed in the United States in 2007," *Archives of Internal Medicine*, vol. 169, no. 22, pp. 2071–2077, Dec. 2009, doi: 10.1001/archinternmed.2009.440.
- [7] UT Southwestern Medical Center, "Diagnostic X-ray procedures." *utswmed.org*, <https://utswmed.org/conditions-treatments/diagnostic-x-ray-procedures/> (accessed Jul. 03, 2020).
- [8] M. B. Freitas, "Dose measurements in chest diagnostic X rays: adult and paediatric patients," *Radiation Protection Dosimetry*, vol. 111, no. 1, pp. 73–76, Aug. 2004, doi: 10.1093/rpd/nch363.
- [9] Siemens-Healthineers, "AX care clear white paper low dose." <https://www.siemens-healthineers.com/it/angio/care-clear> (accessed Nov. 02, 2020).
- [10] A. Sodickson, "Strategies for reducing radiation exposure from multidetector computed tomography in the acute care setting," *Canadian Association of Radiologists Journal*, vol. 64, no. 2, pp. 119–129, May 2013, doi: 10.1016/j.carj.2013.01.002.
- [11] T. ten Cate *et al.*, "Novel X-ray image noise reduction technology reduces patient radiation dose while maintaining image quality in coronary angiography," *Netherlands Heart Journal*, vol. 23, no. 11, pp. 525–530, Nov. 2015, doi: 10.1007/s12471-015-0742-1.
- [12] K. P. Murphy *et al.*, "Feasibility of low-dose CT with model-based iterative image reconstruction in follow-up of patients with testicular cancer," *European Journal of Radiology Open*, vol. 3, pp. 38–45, 2016, doi: 10.1016/j.ejro.2016.01.002.
- [13] B. Luo, Z. Sun, M. Xue, and H. Liu, "Improved noise reduction algorithms for medical X-ray images," in *2013 3rd International Conference on Consumer Electronics, Communications and Networks*, 2013, pp. 359–362, doi: 10.1109/CECNet.2013.6703346.
- [14] P. J. Pickhardt *et al.*, "Abdominal CT with model-based iterative reconstruction (MBIR): initial results of a prospective trial comparing ultralow-dose with standard-dose imaging," *American Journal of Roentgenology*, vol. 199, no. 6, pp. 1266–1274, Dec. 2012, doi: 10.2214/AJR.12.9382.
- [15] X. Wang, A. Sabne, S. Kisner, A. Raghunathan, C. Bouman, and S. Midkiff, "High performance model based image reconstruction," in *Proceedings of the 21st ACM SIGPLAN Symposium on Principles and Practice of Parallel Programming*, Feb. 2016, pp. 1–12, doi: 10.1145/2851141.2851163.
- [16] A. Sabne, X. Wang, S. J. Kisner, C. A. Bouman, A. Raghunathan, and S. P. Midkiff, "Model-based iterative CT image reconstruction on GPUs," in *Proceedings of the 22nd ACM SIGPLAN Symposium on Principles and Practice of Parallel Programming*, Jan. 2017, pp. 207–220, doi: 10.1145/3018743.3018765.
- [17] M. Katsura *et al.*, "Model-based iterative reconstruction technique for radiation dose reduction in chest CT: comparison with the adaptive statistical iterative reconstruction technique," *European Radiology*, vol. 22, no. 8, pp. 1613–1623, Aug. 2012, doi: 10.1007/s00330-012-2452-z.
- [18] H. Scheffel *et al.*, "Coronary artery plaques: Cardiac CT with model-based and adaptive-statistical iterative reconstruction technique," *European Journal of Radiology*, vol. 81, no. 3, pp. e363–e369, Mar. 2012, doi: 10.1016/j.ejrad.2011.11.051.
- [19] Z. Deák *et al.*, "Filtered back projection, adaptive statistical iterative reconstruction, and a model-based Iterative reconstruction in abdominal CT: An experimental clinical study," *Radiology*, vol. 266, no. 1, pp. 197–206, Jan. 2013, doi: 10.1148/radiol.12112707.
- [20] J. Cheng *et al.*, "Model-based deep medical Imaging: the roadmap of generalizing iterative reconstruction model using deep learning," *arXiv:1906.08143*, Jun. 2019.
- [21] H. Chen *et al.*, "Low-dose CT with a residual encoder-decoder convolutional neural network," *IEEE Transactions on Medical Imaging*, vol. 36, no. 12, pp. 2524–2535, Dec. 2017, doi: 10.1109/TMI.2017.2715284.





- [22] N. Kanwal, A. Girdhar, and S. Gupta, "Region based adaptive contrast enhancement of medical X-ray images," in *2011 5th International Conference on Bioinformatics and Biomedical Engineering*, May 2011, pp. 1–5, doi: 10.1109/icbbe.2011.5780221.
- [23] A. Neroladaki, D. Botsikas, S. Boudabbous, C. D. Becker, and X. Montet, "Computed tomography of the chest with model-based iterative reconstruction using a radiation exposure similar to chest X-ray examination: preliminary observations," *European Radiology*, vol. 23, no. 2, pp. 360–366, Feb. 2013, doi: 10.1007/s00330-012-2627-7.
- [24] D. T. Raju and K. Shanthi, "Analysis on x-ray parameters of exposure by measuring x-ray tube voltage and time of exposure," *The International Journal of Engineering and Science (IJES)*, vol. 3, no. 6, pp. 69–73, 2014.
- [25] H. Nien and J. A. Fessler, "Relaxed linearized algorithms for faster X-ray CT image reconstruction," *IEEE Transactions on Medical Imaging*, vol. 35, no. 4, pp. 1090–1098, Apr. 2016, doi: 10.1109/TMI.2015.2508780.
- [26] A. Qadir, "Fluoroscopy dose management." <https://www.slideshare.net/airwave12/patient-radiation-dose-management> (accessed May 18, 2020).
- [27] J. Zhang, Y. Hu, J. Yang, Y. Chen, J.-L. Coatrieux, and L. Luo, "Sparse-view X-ray CT reconstruction with gamma regularization," *Neurocomputing*, vol. 230, pp. 251–269, Mar. 2017, doi: 10.1016/j.neucom.2016.12.019.

BIOGRAPHIES OF AUTHORS



Shama Bekal Narayan     received the B.Eng. degree in Electronics and communication engineering from A.P.S Engineering college, Bangalore, in 2004 and the M.Tech from N.M.A.M. Institute of Technology (NMAMIT) Nitte and pursuing Ph.D. degree from VTU, Belagavi. Currently, she is an Assistant Professor at the Department of Electronics and communication Engineering, St Joseph Engineering College, Mangalore, Karnataka, India. Her research interests include Biomedical image processing, digital circuits, wireless communication, computer communication networks, digital image processing. She can be contacted at shamabn@sjec.ac.in, ResearchGate: <https://www.researchgate.net/profile/Shama-Bekal>.



Savitha Halkare Mahabaleshwara     received her B.E. degree in Electronics and Communication Engineering from Mysore University and her M. Tech. degree in Digital Electronics and Communication from Visvesvaraya Technological University (VTU), Belagavi. She was awarded Doctorate from National Institute of Technology Karnataka (NITK), Surathkal, during April 2014. She has 26 years of teaching experience. She has published around 25 research papers in international journals, international/National conference Proceedings. At savitha100@gmail.com.